JYX JYVÄSKYLÄN YLIOPISTO UNIVERSITY OF JYVÄSKYLÄ

This is a self-archived version of an original article. This version may differ from the original in pagination and typographic details.

Author(s): ALICE Collaboration

Title: Longitudinal and azimuthal evolution of two-particle transverse momentum correlations in Pb–Pb collisions at √sNN = 2.76 TeV

Year: 2020

Version: Published version

Copyright: © 2020 Conseil Européen pour la Recherche Nucléaire

Rights: CC BY 4.0

Rights url: https://creativecommons.org/licenses/by/4.0/

Please cite the original version:

ALICE Collaboration. (2020). Longitudinal and azimuthal evolution of two-particle transverse momentum correlations in Pb–Pb collisions at √sNN = 2.76 TeV. Physics Letters B, 804, Article 135375. https://doi.org/10.1016/j.physletb.2020.135375

Physics Letters B 804 (2020) 135375

Contents lists available at ScienceDirect

Physics Letters B

www.elsevier.com/locate/physletb

Longitudinal and azimuthal evolution of two-particle transverse momentum correlations in Pb–Pb collisions at $\sqrt{s_{\mathrm{NN}}} = 2.76$ TeV

ALICE Collaboration *

ARTICLE INFO

Article history:
Received 16 November 2019
Received in revised form 21 February 2020
Accepted 16 March 2020
Available online 20 March 2020
Editor: M. Doser

ABSTRACT

This paper presents the first measurements of the charge independent (CI) and charge dependent (CD) two-particle transverse momentum correlators G_2^{CI} and G_2^{CD} in Pb–Pb collisions at $\sqrt{s_{\mathrm{NN}}} = 2.76$ TeV by the ALICE collaboration. The two-particle transverse momentum correlator G_2 was introduced as a measure of the momentum current transfer between neighboring system cells. The correlators are measured as a function of pair separation in pseudorapidity ($\Delta\eta$) and azimuth ($\Delta\varphi$) and as a function of collision centrality. From peripheral to central collisions, the correlator G_2^{CI} exhibits a longitudinal broadening while undergoing a monotonic azimuthal narrowing. By contrast, G_2^{CD} exhibits a narrowing along both dimensions. These features are not reproduced by models such as HIJING and AMPT. However, the observed narrowing of the correlators from peripheral to central collisions is expected to result from the stronger transverse flow profiles produced in more central collisions and the longitudinal broadening is predicted to be sensitive to momentum currents and the shear viscosity per unit of entropy density η/s of the matter produced in the collisions. The observed broadening is found to be consistent with the hypothesized lower bound of η/s and is in qualitative agreement with values obtained from anisotropic flow measurements.

© 2020 Conseil Européen pour la Recherche Nucléaire,. Published by Elsevier B.V. This is an open access article under the CC BY license (http://creativecommons.org/licenses/by/4.0/). Funded by SCOAP[3].

1. Introduction

Measurements of particle production and their correlations performed at the Relativistic Heavy Ion Collider (RHIC) and the Large Hadron Collider (LHC) provide compelling evidence that the matter produced in heavy-ion collisions is characterized by extremely high temperatures and energy densities consistent with a deconfined, but strongly interacting Quark–Gluon Plasma (QGP) [1–4]. Collective flow, which manifests itself by the anisotropy of particle production in the plane transverse to the beam direction, is characterized by the harmonic coefficients of a Fourier expansion of the azimuthal distribution of particles relative to the reaction plane. Comparisons of these harmonic coefficients with hydrodynamical model predictions indicate that the matter produced in those collisions has a shear viscosity per unit of entropy density, η/s, that nearly vanishes [2,5]. The shear viscosity quantifies the resistance that any medium presents to its anisotropic deformation. It contributes to the transfer of momentum from one fluid cell to its neighbors as well as the damping of momentum fluctuations. The reach of η/s effects is expected to grow with the lifetime of the system. Recent measurements of flow coefficients and hydrodynamical predictions largely focus on the precise determination of η/s [6–9]. However, quantitative descriptions of heavy-ion collisions with hydrodynamical models generally rely on specific parametrizations of the initial conditions of colliding systems, i.e., their initial energy and entropy density distribution in the transverse plane, the magnitude of initial fluctuations, the thermalization time, and several model parameters. It is found that the precision of model predictions is hindered, in particular, by uncertainties in the initial state conditions. Indeed, values of shear viscosity that best match the observed flow coefficients are dependent on the initial conditions, and unless the magnitude of the initial state fluctuations can be precisely assessed, the achievable precision on η/s might remain limited [10,11]. Systematic studies of correlations between different order harmonic coefficients [12], shown to be sensitive to the initial conditions and the temperature dependence of η/s, can help to provide further constraints to those conditions and to the transport properties of the system. Novel approaches based on Bayesian parameter estimation [13,14] bring progress on a simultaneous characterization of the initial conditions and the QGP. Furthermore, it was pointed out [15] that the strength of momentum current correlations may be sensitive to η/s. It was shown, in particular, that the longitudinal broadening of a transverse momentum (p_{T}) correlator, formally defined below and hereafter named G_2, with increasing system lifetime is directly sensitive to η/s while it does not have any explicit dependence on the initial state fluctuations in the transverse plane of the system.

A first measurement of the broadening of the two-particle transverse momentum correlator G_2 was reported by the STAR

* *E-mail address:* alice-publications@cern.ch.

https://doi.org/10.1016/j.physletb.2020.135375
0370-2693/© 2020 Conseil Européen pour la Recherche Nucléaire,. Published by Elsevier B.V. This is an open access article under the CC BY license (http://creativecommons.org/licenses/by/4.0/). Funded by SCOAP[3].

collaboration [16]. Improved techniques to correct for instrumental effects have since then been reported [17–19]. In this letter, these techniques are used to measure differential charge independent (CI) and charge dependent (CD) two-particle transverse momentum correlators, G_2^{CI} and G_2^{CD}, respectively, as a function of pair rapidity difference, $\Delta\eta$, and azimuthal angle difference, $\Delta\varphi$, for selected ranges of Pb–Pb collision centrality. The shapes of these correlators are studied with a two-component model and the longitudinal and azimuthal widths of their near-side peaks are studied as a function of the Pb–Pb collision centrality. The longitudinal broadening of G_2^{CI} from peripheral to central collisions is used to assess the magnitude of η/s of the matter produced in Pb–Pb collisions while the longitudinal and azimuthal widths of G_2^{CD} are used to assess the role of competing effects, including radial flow, diffusion, and the broadening of jets by interactions with the medium. In that context, measurements of G_2 are also compared with previously reported measurements of the two-particle number correlator R_2 and two-particle transverse momentum correlator P_2 [18].

2. The G_2 correlator

The dimensionless variant of the G_2 correlator [15,20] reported in this letter is defined according to

$$G_2(\eta_1,\varphi_1,\eta_2,\varphi_2) = \frac{1}{\langle p_{\mathrm{T},1}\rangle\langle p_{\mathrm{T},2}\rangle}\left[\frac{\int_\Omega p_{\mathrm{T},1}\,p_{\mathrm{T},2}\,\rho_2(\vec{p}_1,\vec{p}_2)\,\mathrm{d}\,p_{\mathrm{T},1}\mathrm{d}\,p_{\mathrm{T},2}}{\int_\Omega \rho_1(\vec{p}_1)\,\mathrm{d}\,p_{\mathrm{T},1}\int_\Omega \rho_1(\vec{p}_2)\,\mathrm{d}\,p_{\mathrm{T},2}} - \langle p_{\mathrm{T},1}\rangle(\eta_1,\varphi_1)\langle p_{\mathrm{T},2}\rangle(\eta_2,\varphi_2)\right] \quad (1)$$

where Ω is the phase space region in which the measurement is performed; $\vec{p}_1$ and $\vec{p}_2$ are the three-momentum vectors of particles of a given pair; $p_{\mathrm{T},1}$ and $p_{\mathrm{T},2}$ their transverse momentum components, respectively; $\rho_1(\vec{p}_i) = \mathrm{d}^3N/\mathrm{d}p_{\mathrm{T},i}\,\mathrm{d}\eta_i\,\mathrm{d}\varphi_i$ and $\rho_2(\vec{p}_1,\vec{p}_2) = \mathrm{d}^6N/\mathrm{d}p_{\mathrm{T},1}\,\mathrm{d}\eta_1\,\mathrm{d}\varphi_1\,\mathrm{d}p_{\mathrm{T},2}\,\mathrm{d}\eta_2\,\mathrm{d}\varphi_2$ represent single and pair particle densities, expressed as functions of $\vec{p}_i$, $i = 1,2$, and $(\vec{p}_1,\vec{p}_2)$, respectively; $\langle p_{\mathrm{T}}\rangle(\eta_i,\varphi_i)$ is the average transverse momentum of particles observed at (η_i,φ_i), with η_i,φ_i, $i = 1,2$, referring to single-track pseudorapidity and azimuthal angle, respectively; and $\langle p_{\mathrm{T},i}\rangle = \int \rho_1(\vec{p}_i)\,p_{\mathrm{T},i}\,\mathrm{d}\vec{p}_i$ is the inclusive average transverse momentum of produced particles, $i = 1,2$, in the considered event ensemble. Experimentally, G_2 is calculated as

$$G_2(\eta_1,\varphi_1,\eta_2,\varphi_2) = \frac{1}{\langle p_{\mathrm{T},1}\rangle\langle p_{\mathrm{T},2}\rangle}\left[\frac{S_{p_{\mathrm{T}}}(\eta_1,\varphi_1,\eta_2,\varphi_2)}{\langle n_{1,1}(\eta_1,\varphi_1)\rangle\langle n_{1,2}(\eta_2,\varphi_2)\rangle} - \langle p_{\mathrm{T},1}\rangle(\eta_1,\varphi_1)\langle p_{\mathrm{T},2}\rangle(\eta_2,\varphi_2)\right] \quad (2)$$

with

$$S_{p_{\mathrm{T}}}(\eta_1,\varphi_1,\eta_2,\varphi_2) = \left\langle \sum_{\mathrm{i}}^{n_{1,1}}\sum_{\mathrm{j}\neq\mathrm{i}}^{n_{1,2}} p_{\mathrm{T,i}}\,p_{\mathrm{T,j}}\right\rangle \quad (3)$$

where $n_{1,1}$ and $n_{1,2}$ are the number of tracks on each event within bins centered at η_1,φ_1 and η_2,φ_2, and with transverse momentum $p_{\mathrm{T},i}$, $i \in [1,n_{1,1}]$, and $p_{\mathrm{T},j}$, $j \neq i \in [1,n_{1,2}]$, respectively. Angle brackets, $\langle\cdots\rangle$, refer to event ensemble averages, $\langle A\rangle = \sum_1^{N_{\mathrm{events}}} A/N_{\mathrm{events}}$. The correlators G_2^{LS} and G_2^{US} are first measured for like-sign (LS) and unlike-sign (US) pairs separately, and combined to obtain CI and CD correlators according to $G_2^{\mathrm{CI}} = \frac{1}{2}\left(G_2^{\mathrm{US}} + G_2^{\mathrm{LS}}\right)$ and $G_2^{\mathrm{CD}} = \frac{1}{2}\left(G_2^{\mathrm{US}} - G_2^{\mathrm{LS}}\right)$, respectively [18]. Measurements of $G_2(\eta_1,\varphi_1,\eta_2,\varphi_2)$ are averaged across the longitudinal and azimuthal acceptances in which the measurement is performed to obtain $G_2(\Delta\eta,\Delta\varphi)$, where $\Delta\eta = \eta_1 - \eta_2$ and $\Delta\varphi = \varphi_1 - \varphi_2$, with a procedure similar to that used for R_2 and P_2 correlators [18].

3. Measurement techniques

The results presented in this letter are based on 1.1×10^7 selected minimum bias (MB) Pb–Pb collisions at $\sqrt{s_{\mathrm{NN}}}$ = 2.76 TeV collected during the 2010 LHC heavy-ion run by the ALICE experiment. Detailed descriptions of the ALICE detectors and their respective performances are given in Refs. [21,22]. The MB trigger was configured in order to have high efficiency for hadronic events, requiring at least two out of the following three conditions: i) two hits in the second inner layer of the Inner Tracking System (ITS), ii) a signal in the V0A detector, iii) a signal in the V0C detector. The amplitudes measured in the V0 detectors are additionally used to estimate the collision centrality reported in nine classes corresponding to 0–5% (most central), 5–10%, 10–20%, ..., 70–80% (most peripheral) of the total interaction cross section [23]. The vertex position of each collision is determined with tracks reconstructed in the ITS and the Time Projection Chamber (TPC) and is required to be in the range $|z_{\mathrm{vtx}}| \leq 7$ cm of the nominal interaction point (IP). Pile-up events, identified as events having multiple reconstructed vertices in the ITS, are rejected. Additionally, the extra activity observed in slow response detectors (e.g., TPC) relative to that measured in fast detectors (e.g., V0) for out of bunch pile-up events is used to discard these events. The remaining event pile-up contamination is estimated to be negligible. Longitudinally, the ITS covers $|\eta| < 0.9$, the TPC $|\eta| < 0.9$, V0A $2.8 < \eta < 5.1$ and V0C $-3.7 < \eta < -1.7$. These four detectors feature full azimuthal coverage.

The present measurement of the G_2 correlators is based on charged particle tracks measured with the TPC detector in the transverse momentum range $0.2 \leq p_{\mathrm{T}} \leq 2.0$ GeV/c and the pseudorapidity range $|\eta| < 0.8$. In order to ensure good track quality and to minimize secondary track contamination, the analysis is restricted to charged particle tracks involving a minimum of 50 reconstructed TPC space points out of a maximum of 159, and distances of closest approach (DCA) to the reconstructed primary vertex of less than 3.2 cm and 2.4 cm in the longitudinal and radial directions, respectively. An alternative criterion, used in the analysis of the systematic uncertainties, that relies on tracks reconstructed with the combination of the TPC and the ITS detectors, henceforth called "global tracks", involves a minimum of 70 reconstructed TPC space points, hits either on any of two inner layers of the ITS, or in the third inner layer of the ITS, and a tighter DCA selection criterion in both, longitudinal and radial directions, the latter one p_{T}-dependent. Electrons (positrons), whose one of the largest sources are photon conversions into e^+e^- pairs, are suppressed discarding e^+ and e^- by removing tracks with a specific energy loss $\mathrm{d}E/\mathrm{d}x$ in the TPC closer than $3\sigma_{\mathrm{d}E/\mathrm{d}x}$ to the expected median for electrons and at least $5\sigma_{\mathrm{d}E/\mathrm{d}x}$ away from the π, K and p expectation values.

The single and pair efficiencies of the selected charged particles are estimated from a Monte Carlo (MC) simulation using the HIJING event generator [24] with particle transport through the detector performed with GEANT3 [25] tuned to reproduce the detector conditions during the 2010 run. Corrections for single track losses due to non-uniform acceptance (NUA) are carried out using a weighting technique [17] separately for data and for reconstructed MC data. Weights are extracted separately for positive and negative tracks, for each collision centrality range, as a function of η, φ, p_{T} and the longitudinal position of the primary vertex of each event, z_{vtx}. The p_{T}-dependent single track efficiency correction is extracted as the inverse of the ratio of the number of NUA corrected reconstructed HIJING tracks to generated tracks. Data are

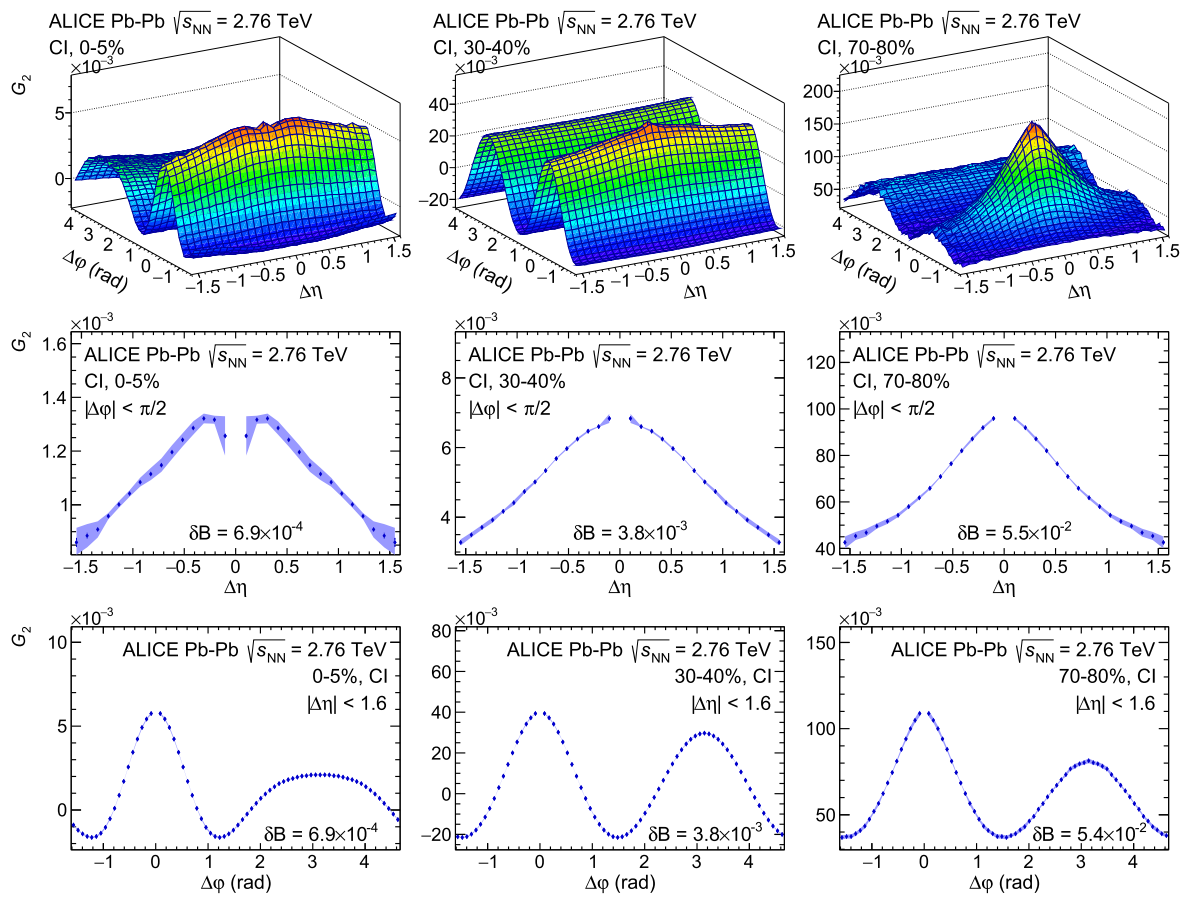

Fig. 1. Two-particle transverse momentum correlations G_2^{CI} (top) and their longitudinal (middle) and azimuthal (bottom) projections for the most central (left), semi-central (center) and peripheral (right) Pb–Pb collisions at $\sqrt{s_{\mathrm{NN}}} = 2.76$ TeV. Vertical bars (mostly smaller than the marker size) and shaded blue bands represent statistical and systematic uncertainties, respectively. The systematic uncertainty on the long-range mean correlator strength is quoted as δB in both projections. Under-corrected correlator values at $\Delta\eta, \Delta\varphi = 0$ are not shown. See text for details.

subsequently corrected with NUA and single track efficiency corrections. Pair losses due to track merging or crossing are corrected in part based on the technique described in [18] and in part based on the ratio of the average number of reconstructed HIJING pairs relative to the generated number of pairs. Corrections for p_{T} dependent pair losses are not included in the reported results given they have a large (> 20%) systematic uncertainty. Correlator values at $|\Delta\eta| < 0.05$, $|\Delta\varphi| < 0.04$ rad., left under-corrected by this last fact, are not reported in this work. However, this does not impact the shape and width of the G_2 correlator, which are of interest for the determination of the viscous broadening. No filters are used to suppress like-sign (LS) particle correlations resulting from Hanbury Brown and Twiss (HBT) effects. For pions, which dominate the particle production, HBT produces a peak centered at $\Delta\eta$, $\Delta\varphi = 0$ in G_2^{LS}. The width of this peak decreases in inverse proportion to the size of the collision system. Given the number of HBT pairs is relatively small compared to the total number of pairs accounted for in G_2^{LS}, the implied reduction of the longitudinal broadening is relatively modest and thus not considered in this analysis.

4. Statistical and systematic uncertainties

Statistical uncertainties on the strength of G_2 are extracted using the sub-sample method with ten sub-samples. Systematic uncertainties are determined by repeating the analysis under different event and track selection conditions. Deviations from the nominal results are considered significant and assessed as systematic uncertainties based on a statistical test [26]. The impact of potential TPC effects sensitive to the magnetic field polarity is assessed by splitting the whole data sample into positive and negative magnetic field configurations, whereas uncertainties associated with the collision centrality estimation are studied by comparing nominal results, based on the V0 detector, with those obtained with an alternative centrality measure based on hit multiplicity on the two inner layers of the ITS. Effects of the kinematic acceptance in which the measurement is performed are investigated by repeating the analysis with events in the range $|z_{\mathrm{vtx}}| < 3$ cm of the nominal IP. The presence of biases caused by secondary particles is checked using the "global tracks" selection criterion. Biases associated with pair losses are studied based on pair efficiency corrections obtained with HIJING/GEANT3 simulations. The largest systematic uncertainty amounts to a global shift in $G_2(\Delta\eta, \Delta\varphi)$ correlator strength which is independent of $\Delta\eta$ and $\Delta\varphi$ and is reported as δB. This shift affects the magnitude of the projections onto $\Delta\eta$ and $\Delta\varphi$ but not the shapes of the near-side peak, $|\Delta\varphi| < \pi/2$, of G_2 along these coordinates. Systematic uncertainties in the shape of the near-side peak of G_2^{CI} and G_2^{CD} are mainly due to the presence of secondary particles. Overall, systematic uncertainties on the shapes of the projections of G_2^{CI} and G_2^{CD} along the longitudinal (azimuthal) dimension amount to 4%(5%) and 5%(10%), respectively, with decreasing values towards peripheral events.

5. Results

Fig. 1 presents the correlators $G_2^{\mathrm{CI}}(\Delta\eta, \Delta\varphi)$ measured in 0–5%, 30–40%, 70–80% Pb–Pb collisions, and their respective projections along the $\Delta\eta$ and $\Delta\varphi$ axes. The G_2^{CI} correlators feature sizable

$\Delta\varphi$ modulations, dominated in mid-central collisions by a strong elliptic flow ($\cos(2\Delta\varphi)$) component. On the near-side, atop the azimuthal modulation, the G_2^{CI} correlators feature a near-side peak whose amplitude monotonically decreases from peripheral to central collisions while its longitudinal width systematically broadens. Qualitatively similar trends were observed for the R_2 and P_2 correlators reported by ALICE [18] and the G_2^{CI} correlator (there named C) reported by STAR [16]. In most central collisions, the amplitude of the $\Delta\varphi$ modulations associated with collective flow decreases but the longitudinal broadening remains. Additionally, a depletion centered at $(\Delta\eta, \Delta\varphi) = (0, 0)$ consistent with previous ALICE results [27,28] can be seen.

In order to study the centrality evolution of the near-side peak of the G_2^{CI} and G_2^{CD} correlators independently of the underlying collective azimuthal behavior, they are separately parametrized with a two-component model defined as

$$F(\Delta\eta, \Delta\varphi) = B + \sum_{n=2}^{6} a_n \times \cos(n\Delta\varphi) + A \times \frac{\gamma_{\Delta\eta}}{2\,\omega_{\Delta\eta}\,\Gamma\left(\frac{1}{\gamma_{\Delta\eta}}\right)} \mathrm{e}^{-\left|\frac{\Delta\eta}{\omega_{\Delta\eta}}\right|^{\gamma_{\Delta\eta}}} \times \frac{\gamma_{\Delta\varphi}}{2\,\omega_{\Delta\varphi}\,\Gamma\left(\frac{1}{\gamma_{\Delta\varphi}}\right)} \mathrm{e}^{-\left|\frac{\Delta\varphi}{\omega_{\Delta\varphi}}\right|^{\gamma_{\Delta\varphi}}}, \quad (4)$$

where B and a_n are intended to describe the long-range mean correlation strength and azimuthal anisotropy, while the bidimensional generalized Gaussian, defined by the parameters A, $\omega_{\Delta\eta}$, $\omega_{\Delta\varphi}$, $\gamma_{\Delta\eta}$ and $\gamma_{\Delta\varphi}$, is intended to model the signal of interest. The $(\Delta\eta, \Delta\varphi) = (0, 0)$ depletion present in the G_2^{CI} correlator is not properly modeled by Eq. (4) and the depletion area, $|\Delta\eta| < 0.31$ and $|\Delta\varphi| < 0.26$ rad., is excluded from the fit. Bidimensional fits are carried out considering only statistical uncertainties. In the case of the G_2^{CI} correlator the χ^2/ndf values for semi-central to peripheral collisions are found in the range 1–2; for central collisions they increase to 4. The area which contributes the most to the increase of the χ^2/ndf is the region between the generalized Gaussian and the Fourier expansion. Excluding this area the χ^2/ndf values obtained in central collisions are within the range 1–2.3. Fits of G_2^{CD} give χ^2/ndf of the order of unity for peripheral to semi-central collisions and in the range 2–3.5 for central collisions. Larger χ^2/ndf values observed in central collisions rise because the near side peak starts to depart from the generalized Gaussian description. The actual focus is on the evolution of the widths. The longitudinal and azimuthal widths of the correlators, denoted $\sigma_{\Delta\eta}$ and $\sigma_{\Delta\varphi}$, respectively, are then extracted as the standard deviation of the generalized Gaussian

$$\sigma_{\Delta\eta(\Delta\varphi)} = \sqrt{\frac{\omega^2_{\Delta\eta(\Delta\varphi)}\Gamma(3/\gamma_{\Delta\eta(\Delta\varphi)})}{\Gamma(1/\gamma_{\Delta\eta(\Delta\varphi)})}}, \quad (5)$$

and plotted as a function of collision centrality in the top panels of Fig. 2 for both G_2^{CI} and G_2^{CD} correlators. The global shift of the correlator strength, quoted as a systematic uncertainty in the projections of the correlators, does not affect the shape of the near-side peak of G_2. Accordingly, the widths are not affected either. Correlations between the contributors to the longitudinal width and the harmonic parameters for the G_2^{CI} correlator are found as follows: a_2 and a_4 are anti-correlated with $\omega_{\Delta\eta}$ with values in the ranges -0.8 to -0.4 and -0.5–0, respectively, while a_3 is correlated with values 0–0.4. On the other hand, a_2 and a_4 are correlated with

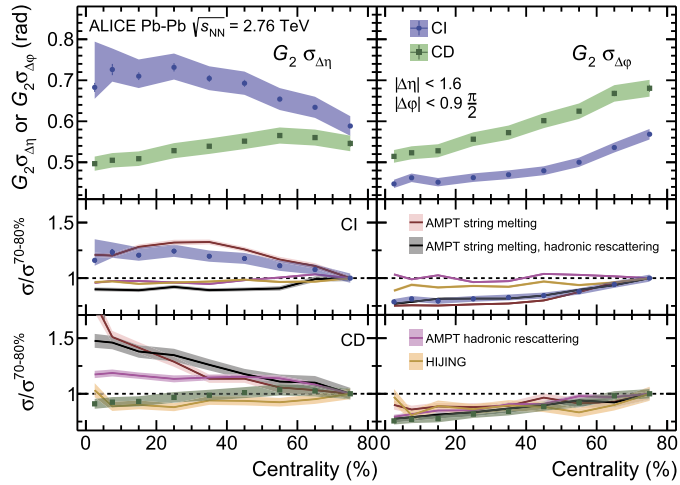

Fig. 2. Top panels: collision centrality evolution of the longitudinal (left) and azimuthal (right) widths of the G_2 CD and CI correlators measured in Pb–Pb collisions at $\sqrt{s_{\mathrm{NN}}} = 2.76$ TeV. Central and bottom panels: width evolution relative to the value in the most peripheral collisions of the two-particle transverse momentum correlations G_2^{CI} (central) and G_2^{CD} (bottom) along the longitudinal (left) and azimuthal (right) dimensions. Data are compared with HIJING and AMPT model expectations. In data, vertical bars and shaded bands represent statistical and systematic uncertainties, respectively. For models, shaded bands represent statistical uncertainties.

$\gamma_{\Delta\eta}$ with values within 0.4–0.8 and 0–0.5, respectively, while a_3 is anti-correlated with values in the range -0.5–0. a_2 correlations show no centrality dependence while the absolute value of a_3 and a_4 correlations decreases from central to peripheral collisions. In the case of the contributors to the azimuthal width, a_2 and a_4 are correlated with $\omega_{\Delta\varphi}$ and with $\gamma_{\Delta\varphi}$ with values in the ranges 0.5–0.8 and 0.6–0.9, and 0.6–0.9 and 0.7–0.9, respectively, while a_3 is anti-correlated with both with values within -0.8 to -0.5 and -0.9 to -0.7. On the azimuthal dimension the absolute value of the harmonic coefficients correlations decreases towards peripheral collisions. Systematic uncertainties in the widths of the near-side peak of G_2^{CI} and G_2^{CD} are mainly due to the presence of secondary particles. With the alternative track selection criterion, systematic uncertainties on the longitudinal and azimuthal widths of the near-side peak are estimated to be 2% and 3%, respectively, for both G_2^{CI} and G_2^{CD}, for most central events, with decreasing values towards peripheral collisions. Uncertainty contributions on the widths are not correlated with centrality and averages along centrality classes are considered. Overall, maximum systematic uncertainties of 4%(2%) and 3.5%(3%) are assigned to the G_2^{CI} and G_2^{CD} widths, respectively, along the longitudinal (azimuthal) dimension. The impact of the size of the area excluded from the fit on the width of the G_2^{CI} correlator is evaluated enlarging the area in both dimensions. Only semi-central to central centrality classes have their corresponding longitudinal widths modified. The effect is a broadening from 1.5% in the 30–40% class up to a broadening of 20% in the 0–5% class incorporated as an additional asymmetric systematic uncertainty on the widths of G_2^{CI}. On the azimuthal widths the impact is reduced to a 2% narrowing.

6. Discussion

Broadening and narrowing are hereafter intended as the behavior of the correlation function, measured by its widths, when going from peripheral collisions, high values of centrality percentile, to central collisions, lower values of centrality percentile. The G_2^{CI} correlator broadens longitudinally but narrows in azimuth, whereas the G_2^{CD} correlator narrows both longitudinally and azimuthally. As shown in Fig. 3, these dependencies are qualitatively consis-

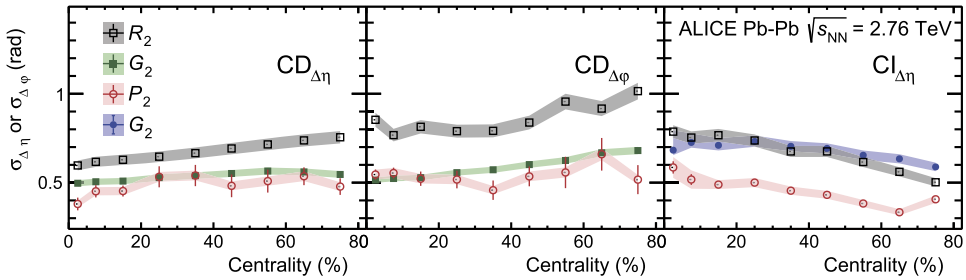

Fig. 3. Left panel: collision centrality evolution of the longitudinal width of number correlator R_2^{CD} and transverse momentum correlators P_2^{CD} and G_2^{CD}. Central panel: idem for the azimuthal width of R_2^{CD}, P_2^{CD} and G_2^{CD}. Right panel: collision centrality evolution of the longitudinal width of R_2^{CI}, P_2^{CI}, and G_2^{CI}. Data for R_2 and P_2 are from [18]. Vertical bars and shaded bands represent statistical and systematic uncertainties, respectively.

tent with those of R_2 and P_2 correlators measured in the same kinematic range by the ALICE collaboration [18]. Note that the G_2 correlator is sensitive to transverse momentum and number density fluctuations since both affect the momentum current density. In contrast, R_2 is sensitive to number density fluctuations and P_2, sensitive to transverse momentum fluctuations, is designed to minimize the contribution of those number density fluctuations [29]. In fact [29]

$$(P_2 + 1)(R_2 + 1) = (G_2 + 1) \tag{6}$$

so, the increase in transverse momentum currents could be due to either the increase in multiplicity or the increase of transverse momentum. The G_2^{CD} and P_2^{CD} correlators feature approximately equal widths while R_2^{CD} is approximately 30% wider throughout its centrality evolution. The centrality dependence of G_2^{CD} is qualitatively consistent with that of balance function (BF) observations [30,31]. Phenomenological analyses of the BFs suggest that their narrowing with centrality is largely due to the presence of strong radial flow and delayed hadronization in Pb–Pb collisions [30]. It is thus reasonable to infer that radial flow and larger $\langle p_T \rangle$, in more central collisions, also produce the observed narrowing of G_2^{CD}. This conjecture is supported by calculations of the collision centrality dependence of G_2^{CD} azimuthal widths with the HIJING and AMPT models shown in the bottom right panel of Fig. 2. Radial flow might also explain the observed azimuthal narrowing of the G_2^{CI} correlator with centrality, which is reasonably well reproduced by calculations with AMPT with string melting, but not by HIJING or AMPT calculations with only hadronic rescattering as shown in central right panel of Fig. 2.

The broadening of the longitudinal width of the G_2^{CI} correlator is of particular interest given predictions that it should grow in proportion to η/s of the matter produced in the collisions [15]. As expected for a system with finite viscosity, it is found that G_2^{CI} broadens significantly with increasing collision centrality, while by contrast, G_2^{CD} exhibits a slight but distinct narrowing. This G_2^{CD} longitudinal narrowing is expected from a boost of particle pairs by radial flow but is not properly accounted for by AMPT calculations shown in the bottom left panel of Fig. 2. Radial flow should also produce a narrowing of the G_2^{CI} correlator in the longitudinal direction. However competing effects, possibly associated with the finite shear viscosity of the system, are instead producing a significant broadening although reaching what seems a saturation level at semi-central collisions. Note that HIJING and AMPT, with the hadronic rescattering enabled, grossly fail to reproduce the observed broadening and instead predict a slight narrowing (Fig. 2 central left panel). AMPT with string melting and without the hadronic rescattering phase qualitatively reproduces the longitudinal broadening of G_2^{CI}, even its saturation, but grossly miss the narrowing of G_2^{CD} along that dimension and thus cannot be considered reliable in this context.

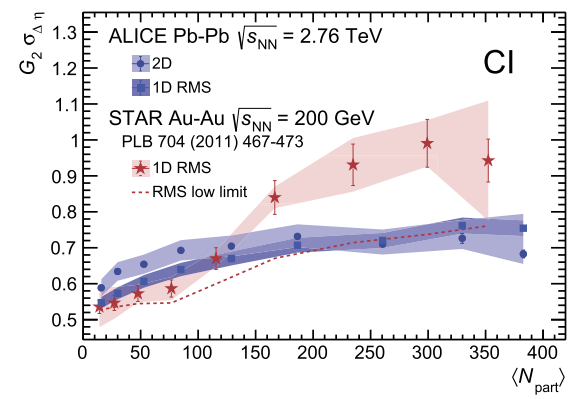

Fig. 4. Two-particle transverse momentum correlation G_2^{CI} longitudinal width evolution with the number of participants in Au–Au collisions at $\sqrt{s_{NN}} = 200$ GeV [16] and in Pb–Pb collisions at $\sqrt{s_{NN}} = 2.76$ TeV, measured in this work, using the bi-dimensional fit described in the text (2D) and the method used by the STAR experiment [16] (1D). For completeness, STAR RMS low limit [16] is also shown.

Particles produced by jet fragmentation are also known to exhibit correlations and jet-medium interactions can broaden such correlations. Two-particle correlation measurements, of particles associated with high-p_T jets, indeed show substantial broadening of low p_T particle correlations relative to correlation functions measured in pp collisions [27,28,32]. This broadening, however, is observed in both the longitudinal and azimuthal directions in stark contrast with the behavior of the inclusive G_2^{CI} correlator measured in this work which exhibits a significant narrowing in the azimuthal direction. Additionally, the number of particles from jets is relatively small compared to the number from the bulk. Therefore, although jet fragmentation may contribute to the broadening observed in the longitudinal direction, it is unlikely to amount to a significant contribution given the observed narrowing in the $\Delta\varphi$ direction and the relatively low impact of correlations from jet particles.

Fig. 4 compares results from this analysis with those reported by the STAR collaboration [16]. For proper comparison, Fig. 4 presents root mean square (RMS) widths of $\Delta\eta$ projections of G_2^{CI} calculated above a long range baseline as in the STAR analysis [16]. Although STAR reported results are based on the dimensional version of G_2^{CI}, the same expression as in Eq. (1) but without the normalization $\langle p_{T,1} \rangle \langle p_{T,2} \rangle$, the correlator widths reported in this letter are identical for both, the dimensional and dimensionless versions of the G_2 correlator. The longitudinal broadening measured in this analysis, using the 1D RMS method, amounts to 36% while that observed by STAR reaches 74% showing also a saturation at semi-central collisions. It was verified that the smaller broadening seen in this analysis is not a result of the slightly narrower longitudinal acceptance of the ALICE experiment by testing the analysis method with Monte Carlo models reproducing the approximate shape and strength of the measured correlation functions. The longitudinal

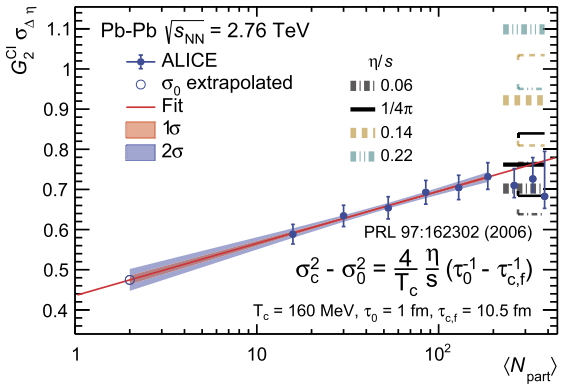

Fig. 5. Expected longitudinal widths for the most central collisions of the two-particle transverse momentum correlation G_2^{CI} for different values of η/s by using the expression suggested in [15]. Data point error bars represent total uncertainties obtained by adding in quadrature statistical and systematic uncertainties. In the formula σ_c is the longitudinal width for the most central collisions inferred by using this expression and represented for each of the η/s values by the color discontinuous bands (continuous for $\eta/s = 1/4\pi$) at the highest number of participants, σ_0 is the longitudinal width for the most peripheral collisions (only two participants) which is obtained by extrapolating the fit, T_c is the critical temperature, τ_0 is the formation time and $\tau_{c,f}$ the freeze-out time. Error caps in the same color as the discontinuous bands, represent uncertainties of the inferred longitudinal widths for the most central collisions (see text for details).

broadening of G_2^{CI} and its observed saturation thus appears to be potentially dependent on the beam energy.

Interpreting the longitudinal broadening of G_2^{CI} as originating exclusively from viscous effects, an estimate of the shear viscosity per unit of entropy density, η/s, of the matter produced in heavy-ion collisions can be extracted [16] using the expression

$$\sigma_c^2 - \sigma_0^2 = \frac{4}{T_c}\frac{\eta}{s}\left(\frac{1}{\tau_0} - \frac{1}{\tau_{c,f}}\right) \tag{7}$$

derived in [15]. In Eq. (7) σ_c is the longitudinal width for the most central collisions (ideally 0% centrality), σ_0 is the longitudinal width for the most peripheral collisions (ideally 100% centrality), T_c is the critical temperature, τ_0 is the formation time and $\tau_{c,f}$ the freeze-out time. The correlator width for the most peripheral Pb–Pb collisions at $\sqrt{s_{NN}} = 2.76$ TeV is estimated based on a power law extrapolation of the measured values, shown in Fig. 5, down to $N_{\mathrm{part}} = 2$. Canonical values are used for the critical temperature, $T_c = 160$ MeV [33], the formation time $\tau_0 = 1$ fm/c [33], and the freeze-out time, $\tau_{c,f} = 10.5$ fm/c [34]. With these inputs in Eq. (7), G_2^{CI} longitudinal widths for the most central collisions are calculated for several values of $\eta/s = 0.06$, $1/4\pi$, 0.14 and 0.22 and also shown in Fig. 5 as color discontinuous (continuous for $\eta/s = 1/4\pi$) bands at the highest number of participants. Considering 2%, 30%, and 3% uncertainties for T_c ($155 < T_c < 165$ TeV), τ_0, and $\tau_{c,f}$ ($10 < \tau_{c,f} < 11$ fm) respectively, the uncertainties of the four obtained G_2^{CI} longitudinal widths for the most central collisions reach 9%, 10%, 12%, and 14%, respectively, also shown in Fig. 5 as error caps in the same color as the discontinuous bands. The G_2^{CI} correlator width measured in central collisions thus favors rather small values of η/s, close to the KSS limit of $1/4\pi$ [35]. The authors of Ref. [15] obtain the correlator width values, for Au–Au collisions at $\sqrt{s_{NN}} = 200$ GeV, without an actual measurement of G_2^{CI} from the only available two-particle transverse momentum correlator which in its turn was inferred from event-wise mean transverse momentum fluctuations [36] and on its energy dependence [37]. They constrain η/s to a relatively wide interval 0.08–0.30. The precision of the STAR measurement is limited by the relative uncertainty of the G_2^{CI} correlator widths for Au–Au collisions at $\sqrt{s_{NN}} = 200$ GeV; $\eta/s = 0.06$–0.21 was reported in [16].

7. Conclusions

Measurements of charge dependent (CD) and charge independent (CI) transverse momentum correlators G_2 in Pb–Pb collisions at $\sqrt{s_{NN}} = 2.76$ TeV were presented aiming at the determination of the shear viscosity per unit of entropy density, η/s, of the matter formed in such collisions. The near-side peak of the G_2^{CD} correlator is observed to significantly narrow with collision centrality both in the longitudinal and azimuthal directions. This behavior is found to be similar to that of the charge balance function as a result, most likely, of an increase of the average radial flow velocity from peripheral to central collisions. By contrast, the G_2^{CI} correlator is found to narrow only in the azimuthal direction with collision centrality and features a sizable broadening in the longitudinal direction. The observed broadening along the longitudinal direction is expected based on friction forces associated with the finite shear viscosity of the system. Taking the model proposed in [15], an estimate of the value of η/s of order $1/4\pi$, in qualitative agreement with values obtained from other methods [14,38], is obtained. String melting AMPT without the hadronic rescattering phase has been found to qualitatively reproduce the longitudinal broadening of G_2^{CI} but grossly misses the narrowing of G_2^{CD} along that dimension. The observed saturation in the longitudinal broadening and the sizable difference in broadening relative to that observed by STAR may result from the interplay of viscous forces and kinematic narrowing associated to radial flow. In the latter case, the difference compared to the STAR results due to a possible dependence on the beam energy could be better established with expanded experimental measurements for energies in the beam energy scan (BES) at RHIC or at 5.02 TeV at the LHC.

Declaration of competing interest

The authors declare that they have no known competing financial interests or personal relationships that could have appeared to influence the work reported in this paper.

Acknowledgements

Authors thank Dr. Sean Gavin and Dr. George Moschelli for fruitful discussions.

The ALICE Collaboration would like to thank all its engineers and technicians for their invaluable contributions to the construction of the experiment and the CERN accelerator teams for the outstanding performance of the LHC complex. The ALICE Collaboration gratefully acknowledges the resources and support provided by all Grid centres and the Worldwide LHC Computing Grid (WLCG) collaboration. The ALICE Collaboration acknowledges the following funding agencies for their support in building and running the ALICE detector: A. I. Alikhanyan National Science Laboratory (Yerevan Physics Institute) Foundation (ANSL), State Committee of Science and World Federation of Scientists (WFS), Armenia; Austrian Academy of Sciences, Austrian Science Fund (FWF): [M 2467-N36] and Nationalstiftung für Forschung, Technologie und Entwicklung, Austria; Ministry of Communications and High Technologies, National Nuclear Research Center, Azerbaijan; Conselho Nacional de Desenvolvimento Científico e Tecnológico (CNPq), Financiadora de Estudos e Projetos (Finep), Fundação de Amparo à Pesquisa do Estado de São Paulo (FAPESP) and Universidade Federal do Rio Grande do Sul (UFRGS), Brazil; Ministry of Education of China (MOEC), Ministry of Science & Technology of China (MSTC) and National Natural Science Foundation of China (NSFC), China; Ministry of Science and Education and Croatian Science Foundation, Croatia; Centro de Aplicaciones Tecnológicas y Desarrollo Nuclear (CEADEN), Cubaenergía, Cuba; Ministry of Education, Youth and Sports of the Czech Republic, Czech Republic; The Danish Council

for Independent Research|Natural Sciences, the Villum Fonden and Danish National Research Foundation (DNRF), Denmark; Helsinki Institute of Physics (HIP), Finland; Commissariat à l'Energie Atomique (CEA), Institut National de Physique Nucléaire et de Physique des Particules (IN2P3) and Centre National de la Recherche Scientifique (CNRS) and Région des Pays de la Loire, France; Bundesministerium für Bildung und Forschung (BMBF) and GSI Helmholtzzentrum für Schwerionenforschung GmbH, Germany; General Secretariat for Research and Technology, Ministry of Education, Research and Religions, Greece; National Research, Development and Innovation Office, Hungary; Department of Atomic Energy, Government of India (DAE), Department of Science and Technology, Government of India (DST), University Grants Commission, Government of India (UGC) and Council of Scientific and Industrial Research (CSIR), India; Indonesian Institute of Science, Indonesia; Centro Fermi - Museo Storico della Fisica e Centro Studi e Ricerche Enrico Fermi and Instituto Nazionale di Fisica Nucleare (INFN), Italy; Institute for Innovative Science and Technology, Nagasaki Institute of Applied Science (IIST), Japanese Ministry of Education, Culture, Sports, Science and Technology (MEXT) and Japan Society for the Promotion of Science (JSPS) KAKENHI, Japan; Consejo Nacional de Ciencia (CONACYT) y Tecnología, through Fondo de Cooperación Internacional en Ciencia y Tecnología (FONCICYT) and Dirección General de Asuntos del Personal Academico (DGAPA), Mexico; Nederlandse Organisatie voor Wetenschappelijk Onderzoek (NWO), Netherlands; The Research Council of Norway, Norway; Commission on Science and Technology for Sustainable Development in the South (COMSATS), Pakistan; Pontificia Universidad Católica del Perú, Peru; Ministry of Science and Higher Education and National Science Centre, Poland; Korea Institute of Science and Technology Information and National Research Foundation of Korea (NRF), Republic of Korea; Ministry of Education and Scientific Research, Institute of Atomic Physics and Ministry of Research and Innovation and Institute of Atomic Physics, Romania; Joint Institute for Nuclear Research (JINR), Ministry of Education and Science of the Russian Federation, National Research Centre Kurchatov Institute, Russian Science Foundation and Russian Foundation for Basic Research, Russia; Ministry of Education, Science, Research and Sport of the Slovak Republic, Slovakia; National Research Foundation of South Africa, South Africa; Swedish Research Council (VR) and Knut & Alice Wallenberg Foundation (KAW), Sweden; European Organization for Nuclear Research, Switzerland; Suranaree University of Technology (SUT), National Science and Technology Development Agency (NSDTA) and Office of the Higher Education Commission under NRU project of Thailand, Thailand; Turkish Atomic Energy Authority (TAEK), Turkey; National Academy of Sciences of Ukraine, Ukraine; Science and Technology Facilities Council (STFC), United Kingdom; National Science Foundation of the United States of America (NSF) and United States Department of Energy, Office of Nuclear Physics (DOE NP), United States of America.

References

[1] STAR Collaboration, J. Adams, et al., Experimental and theoretical challenges in the search for the quark gluon plasma: the STAR Collaboration's critical assessment of the evidence from RHIC collisions, Nucl. Phys. A 757 (2005) 102–183, arXiv:nucl-ex/0501009 [nucl-ex].

[2] PHENIX Collaboration, K. Adcox, et al., Formation of dense partonic matter in relativistic nucleus-nucleus collisions at RHIC: experimental evaluation by the PHENIX Collaboration, Nucl. Phys. A 757 (2005) 184–283, arXiv:nucl-ex/0410003 [nucl-ex].

[3] BRAHMS Collaboration, I. Arsene, et al., Quark gluon plasma and color glass condensate at RHIC? The perspective from the BRAHMS experiment, Nucl. Phys. A 757 (12) (2005) 1–27, http://www.sciencedirect.com/science/article/pii/S0375947405002770, First Three Years of Operation of RHIC.

[4] PHOBOS Collaboration, B.B. Back, et al., The PHOBOS perspective on discoveries at RHIC, Nucl. Phys. A 757 (2005) 28–101, arXiv:nucl-ex/0410022 [nucl-ex].

[5] U. Heinz, C. Shen, H. Song, The viscosity of quark-gluon plasma at RHIC and the LHC, AIP Conf. Proc. 1441 (1) (2012) 766–770, arXiv:1108.5323 [nucl-th].

[6] STAR Collaboration, J. Adams, et al., Azimuthal anisotropy in Au+Au collisions at $\sqrt{s_{NN}} = 200$ GeV, Phys. Rev. C 72 (2005) 014904, arXiv:nucl-ex/0409033 [nucl-ex].

[7] ALICE Collaboration, K. Aamodt, et al., Harmonic decomposition of two-particle angular correlations in Pb–Pb collisions at $\sqrt{s_{NN}} = 2.76$ TeV, Phys. Lett. B 708 (2012) 249–264, arXiv:1109.2501 [nucl-ex].

[8] U. Heinz, R. Snellings, Collective flow and viscosity in relativistic heavy-ion collisions, Annu. Rev. Nucl. Part. Sci. 63 (2013) 123–151, arXiv:1301.2826 [nucl-th].

[9] ALICE Collaboration, K. Aamodt, et al., Elliptic flow of charged particles in Pb–Pb collisions at 2.76 TeV, Phys. Rev. Lett. 105 (2010) 252302, arXiv:1011.3914 [nucl-ex].

[10] H. Song, S.A. Bass, U. Heinz, T. Hirano, C. Shen, 200 A GeV Au+Au collisions serve a nearly perfect quark-gluon liquid, Phys. Rev. Lett. 106 (2011) 192301, arXiv:1011.2783, Erratum: Phys. Rev. Lett. 109 (2012) 139904.

[11] C. Shen, U. Heinz, Collision energy dependence of viscous hydrodynamic flow in relativistic heavy-ion collisions, Phys. Rev. C 85 (2012) 054902, arXiv:1202.6620 [nucl-th], Erratum: Phys. Rev. C 86 (2012) 049903.

[12] ALICE Collaboration, S. Acharya, et al., Systematic studies of correlations between different order flow harmonics in Pb–Pb collisions at $\sqrt{s_{NN}} = 2.76$ TeV, Phys. Rev. C 97 (2) (2018) 024906, arXiv:1709.01127 [nucl-ex].

[13] J. Auvinen, J.E. Bernhard, S.A. Bass, I. Karpenko, Investigating the collision energy dependence of η/s in the beam energy scan at the BNL relativistic heavy ion collider using Bayesian statistics, Phys. Rev. C 97 (Apr 2018) 044905, https://link.aps.org/doi/10.1103/PhysRevC.97.044905.

[14] J.E. Bernhard, J.S. Moreland, S.A. Bass, J. Liu, U. Heinz, Applying Bayesian parameter estimation to relativistic heavy-ion collisions: simultaneous characterization of the initial state and quark-gluon plasma medium, Phys. Rev. C 94 (2) (2016) 024907, arXiv:1605.03954 [nucl-th].

[15] S. Gavin, M. Abdel-Aziz, Measuring shear viscosity using transverse momentum correlations in relativistic nuclear collisions, Phys. Rev. Lett. 97 (2006) 162302, arXiv:nucl-th/0606061 [nucl-th].

[16] STAR Collaboration, G. Agakishiev, et al., Evolution of the differential transverse momentum correlation function with centrality in Au+Au collisions at $\sqrt{s_{NN}} = 200$ GeV, Phys. Lett. B 704 (2011) 467–473, arXiv:1106.4334 [nucl-ex].

[17] S. Ravan, P. Pujahari, S. Prasad, C.A. Pruneau, Correcting correlation function measurements, Phys. Rev. C 89 (2) (2014) 024906, arXiv:1311.3915 [nucl-ex].

[18] ALICE Collaboration, S. Acharya, et al., Two-particle differential transverse momentum and number density correlations in p–Pb and Pb–Pb at the LHC, Phys. Rev. C 100 (Oct 2019) 044903, arXiv:1805.04422 [nucl-ex].

[19] V. Gonzalez, A. Marin, P. Ladron De Guevara, J. Pan, S. Basu, C. Pruneau, Effect of centrality bin width corrections on two-particle number and transverse momentum differential correlation functions, Phys. Rev. C 99 (3) (2019) 034907, arXiv:1809.04962 [physics.data-an].

[20] M. Sharma, C.A. Pruneau, Methods for the study of transverse momentum differential correlations, Phys. Rev. C 79 (2009) 024905, arXiv:0810.0716 [nucl-ex].

[21] ALICE Collaboration, K. Aamodt, et al., The Alice experiment at the CERN LHC, J. Instrum. 3 (08) (2008), S08002, http://stacks.iop.org/1748-0221/3/i=08/a=S08002.

[22] ALICE Collaboration, B. Abelev, et al., Performance of the Alice experiment at the CERN LHC, Int. J. Mod. Phys. A 29 (2014) 1430044, arXiv:1402.4476 [nucl-ex].

[23] ALICE Collaboration, B. Abelev, et al., Centrality determination of Pb–Pb collisions at $\sqrt{s_{NN}} = 2.76$ TeV with Alice, Phys. Rev. C 88 (4) (2013) 044909, arXiv:1301.4361 [nucl-ex].

[24] X.-N. Wang, M. Gyulassy, HIJING: a Monte Carlo model for multiple jet production in p p, p A and A A collisions, Phys. Rev. D 44 (1991) 3501–3516.

[25] R. Brun, F. Bruyant, F. Carminati, S. Giani, M. Maire, A. McPherson, G. Patrick, L. Urban, GEANT: Detector Description and Simulation Tool, Oct 1994, CERN Program Library, CERN, Geneva, 1993, http://cds.cern.ch/record/1082634, Long Writeup W5013.

[26] R. Barlow, Systematic errors: facts and fictions, in: Advanced Statistical Techniques in Particle Physics, Proceedings, Conference, Durham, UK, March 18-22, 2002, 2002, pp. 134–144, arXiv:hep-ex/0207026 [hep-ex], http://www.ippp.dur.ac.uk/Workshops/02/statistics/proceedings//barlow.pdf.

[27] ALICE Collaboration, J. Adam, et al., Anomalous evolution of the near-side jet peak shape in Pb–Pb collisions at $\sqrt{s_{NN}} = 2.76$ TeV, Phys. Rev. Lett. 119 (10) (2017) 102301, arXiv:1609.06643 [nucl-ex].

[28] ALICE Collaboration, J. Adam, et al., Evolution of the longitudinal and azimuthal structure of the near-side jet peak in Pb–Pb collisions at $\sqrt{s_{NN}} = 2.76$ TeV, Phys. Rev. C 96 (3) (2017) 034904, arXiv:1609.06667 [nucl-ex].

[29] S. Gavin, G. Moschelli, Viscosity and the soft ridge at RHIC, J. Phys. G 35 (2008) 104084, arXiv:0806.4366 [nucl-th].

[30] ALICE Collaboration, B. Abelev, et al., Charge correlations using the balance function in Pb–Pb collisions at $\sqrt{s_{NN}} = 2.76$ TeV, Phys. Lett. B 723 (2013) 267–279, arXiv:1301.3756 [nucl-ex].

[31] ALICE Collaboration, J. Adam, et al., Multiplicity and transverse momentum evolution of charge-dependent correlations in pp, p–Pb, and Pb–Pb collisions at the LHC, Eur. Phys. J. C 76 (2) (2016) 86, arXiv:1509.07255 [nucl-ex].

[32] CMS Collaboration, S. Chatrchyan, et al., Measurement of jet fragmentation in PbPb and pp collisions at $\sqrt{s_{NN}} = 2.76$ TeV, Phys. Rev. C 90 (2) (2014) 024908, arXiv:1406.0932 [nucl-ex].

[33] F. Becattini, The quark gluon plasma and relativistic heavy ion collisions in the LHC era, J. Phys. Conf. Ser. 527 (2014) 012012.

[34] ALICE Collaboration, K. Aamodt, et al., Two-pion Bose-Einstein correlations in central Pb–Pb collisions at $\sqrt{s_{NN}}$ = 2.76 TeV, Phys. Lett. B 696 (2011) 328–337, arXiv:1012.4035 [nucl-ex].

[35] P. Kovtun, D.T. Son, A.O. Starinets, Viscosity in strongly interacting quantum field theories from black hole physics, Phys. Rev. Lett. 94 (2005) 111601, arXiv:hep-th/0405231 [hep-th].

[36] STAR Collaboration, J. Adams, et al., Transverse-momentum p_T correlations on (η, φ) from mean-p_T fluctuations in Au–Au collisions at $\sqrt{s_{NN}} = 200$ GeV, J. Phys. G 32 (2006) L37–L48, arXiv:nucl-ex/0509030 [nucl-ex].

[37] STAR Collaboration, J. Adams, et al., The energy dependence of p_T angular correlations inferred from mean-p_T fluctuation scale dependence in heavy ion collisions at the SPS and RHIC, J. Phys. G 34 (2007) 451–466, arXiv:nucl-ex/0605021 [nucl-ex].

[38] J.S. Moreland, J.E. Bernhard, S.A. Bass, Estimating initial state and quark-gluon plasma medium properties using a hybrid model with nucleon substructure calibrated to p-Pb and Pb–Pb collisions at $\sqrt{s_{NN}} = 5.02$ TeV, arXiv:1808.02106 [nucl-th].

ALICE Collaboration

S. Acharya [141], D. Adamová [94], A. Adler [74], J. Adolfsson [80], M.M. Aggarwal [99], G. Aglieri Rinella [33], M. Agnello [30], N. Agrawal [10,53], Z. Ahammed [141], S. Ahmad [16], S.U. Ahn [76], A. Akindinov [91], M. Al-Turany [106], S.N. Alam [141], D.S.D. Albuquerque [122], D. Aleksandrov [87], B. Alessandro [58], H.M. Alfanda [6], R. Alfaro Molina [71], B. Ali [16], Y. Ali [14], A. Alici [10,26,53], A. Alkin [2], J. Alme [21], T. Alt [68], L. Altenkamper [21], I. Altsybeev [112], M.N. Anaam [6], C. Andrei [47], D. Andreou [33], H.A. Andrews [110], A. Andronic [144], M. Angeletti [33], V. Anguelov [103], C. Anson [15], T. Antičić [107], F. Antinori [56], P. Antonioli [53], R. Anwar [125], N. Apadula [79], L. Aphecetche [114], H. Appelshäuser [68], S. Arcelli [26], R. Arnaldi [58], M. Arratia [79], I.C. Arsene [20], M. Arslandok [103], A. Augustinus [33], R. Averbeck [106], S. Aziz [61], M.D. Azmi [16], A. Badalà [55], Y.W. Baek [40], S. Bagnasco [58], X. Bai [106], R. Bailhache [68], R. Bala [100], A. Baldisseri [137], M. Ball [42], S. Balouza [104], R. Barbera [27], L. Barioglio [25], G.G. Barnaföldi [145], L.S. Barnby [93], V. Barret [134], P. Bartalini [6], K. Barth [33], E. Bartsch [68], F. Baruffaldi [28], N. Bastid [134], S. Basu [143], G. Batigne [114], B. Batyunya [75], D. Bauri [48], J.L. Bazo Alba [111], I.G. Bearden [88], C. Bedda [63], N.K. Behera [60], I. Belikov [136], A.D.C. Bell Hechavarria [144], F. Bellini [33], R. Bellwied [125], V. Belyaev [92], G. Bencedi [145], S. Beole [25], A. Bercuci [47], Y. Berdnikov [97], D. Berenyi [145], R.A. Bertens [130], D. Berzano [58], M.G. Besoiu [67], L. Betev [33], A. Bhasin [100], I.R. Bhat [100], M.A. Bhat [3], H. Bhatt [48], B. Bhattacharjee [41], A. Bianchi [25], L. Bianchi [25], N. Bianchi [51], J. Bielčík [36], J. Bielčíková [94], A. Bilandzic [104,117], G. Biro [145], R. Biswas [3], S. Biswas [3], J.T. Blair [119], D. Blau [87], C. Blume [68], G. Boca [139], F. Bock [33,95], A. Bogdanov [92], S. Boi [23], L. Boldizsár [145], A. Bolozdynya [92], M. Bombara [37], G. Bonomi [140], H. Borel [137], A. Borissov [92,144], H. Bossi [146], E. Botta [25], L. Bratrud [68], P. Braun-Munzinger [106], M. Bregant [121], M. Broz [36], E.J. Brucken [43], E. Bruna [58], G.E. Bruno [105], M.D. Buckland [127], D. Budnikov [108], H. Buesching [68], S. Bufalino [30], O. Bugnon [114], P. Buhler [113], P. Buncic [33], Z. Buthelezi [72,131], J.B. Butt [14], J.T. Buxton [96], S.A. Bysiak [118], D. Caffarri [89], A. Caliva [106], E. Calvo Villar [111], R.S. Camacho [44], P. Camerini [24], A.A. Capon [113], F. Carnesecchi [10,26], R. Caron [137], J. Castillo Castellanos [137], A.J. Castro [130], E.A.R. Casula [54], F. Catalano [30], C. Ceballos Sanchez [52], P. Chakraborty [48], S. Chandra [141], W. Chang [6], S. Chapeland [33], M. Chartier [127], S. Chattopadhyay [141], S. Chattopadhyay [109], A. Chauvin [23], C. Cheshkov [135], B. Cheynis [135], V. Chibante Barroso [33], D.D. Chinellato [122], S. Cho [60], P. Chochula [33], T. Chowdhury [134], P. Christakoglou [89], C.H. Christensen [88], P. Christiansen [80], T. Chujo [133], C. Cicalo [54], L. Cifarelli [10,26], F. Cindolo [53], J. Cleymans [124], F. Colamaria [52], D. Colella [52], A. Collu [79], M. Colocci [26], M. Concas [58,ii], G. Conesa Balbastre [78], Z. Conesa del Valle [61], G. Contin [24,127], J.G. Contreras [36], T.M. Cormier [95], Y. Corrales Morales [25], P. Cortese [31], M.R. Cosentino [123], F. Costa [33], S. Costanza [139], P. Crochet [134], E. Cuautle [69], P. Cui [6], L. Cunqueiro [95], D. Dabrowski [142], T. Dahms [104,117], A. Dainese [56], F.P.A. Damas [114,137], M.C. Danisch [103], A. Danu [67], D. Das [109], I. Das [109], P. Das [85], P. Das [3], S. Das [3], A. Dash [85], S. Dash [48], S. De [85], A. De Caro [29], G. de Cataldo [52], J. de Cuveland [38], A. De Falco [23], D. De Gruttola [10], N. De Marco [58], S. De Pasquale [29], S. Deb [49], B. Debjani [3], H.F. Degenhardt [121], K.R. Deja [142], A. Deloff [84], S. Delsanto [25,131], D. Devetak [106], P. Dhankher [48], D. Di Bari [32], A. Di Mauro [33], R.A. Diaz [8], T. Dietel [124], P. Dillenseger [68], Y. Ding [6], R. Divià [33], D.U. Dixit [19], Ø. Djuvsland [21], U. Dmitrieva [62], A. Dobrin [33,67], B. Dönigus [68], O. Dordic [20], A.K. Dubey [141], A. Dubla [106], S. Dudi [99], M. Dukhishyam [85], P. Dupieux [134], R.J. Ehlers [146], V.N. Eikeland [21], D. Elia [52], H. Engel [74], E. Epple [146], B. Erazmus [114], F. Erhardt [98], A. Erokhin [112], M.R. Ersdal [21], B. Espagnon [61], G. Eulisse [33], D. Evans [110], S. Evdokimov [90], L. Fabbietti [104,117], M. Faggin [28], J. Faivre [78], F. Fan [6], A. Fantoni [51], M. Fasel [95], P. Fecchio [30], A. Feliciello [58], G. Feofilov [112], A. Fernández Téllez [44], A. Ferrero [137], A. Ferretti [25], A. Festanti [33], V.J.G. Feuillard [103], J. Figiel [118], S. Filchagin [108], D. Finogeev [62], F.M. Fionda [21], G. Fiorenza [52],

F. Flor [125], S. Foertsch [72], P. Foka [106], S. Fokin [87], E. Fragiacomo [59], U. Frankenfeld [106], U. Fuchs [33], C. Furget [78], A. Furs [62], M. Fusco Girard [29], J.J. Gaardhøje [88], M. Gagliardi [25], A.M. Gago [111], A. Gal [136], C.D. Galvan [120], P. Ganoti [83], C. Garabatos [106], E. Garcia-Solis [11], K. Garg [27], C. Gargiulo [33], A. Garibli [86], K. Garner [144], P. Gasik [104,117], E.F. Gauger [119], M.B. Gay Ducati [70], M. Germain [114], J. Ghosh [109], P. Ghosh [141], S.K. Ghosh [3], P. Gianotti [51], P. Giubellino [58,106], P. Giubilato [28], P. Glässel [103], D.M. Goméz Coral [71], A. Gomez Ramirez [74], V. Gonzalez [106], P. González-Zamora [44], S. Gorbunov [38], L. Görlich [118], S. Gotovac [34], V. Grabski [71], L.K. Graczykowski [142], K.L. Graham [110], L. Greiner [79], A. Grelli [63], C. Grigoras [33], V. Grigoriev [92], A. Grigoryan [1], S. Grigoryan [75], O.S. Groettvik [21], F. Grosa [30], J.F. Grosse-Oetringhaus [33], R. Grosso [106], R. Guernane [78], M. Guittiere [114], K. Gulbrandsen [88], T. Gunji [132], A. Gupta [100], R. Gupta [100], I.B. Guzman [44], R. Haake [146], M.K. Habib [106], C. Hadjidakis [61], H. Hamagaki [81], G. Hamar [145], M. Hamid [6], R. Hannigan [119], M.R. Haque [63,85], A. Harlenderova [106], J.W. Harris [146], A. Harton [11], J.A. Hasenbichler [33], H. Hassan [95], D. Hatzifotiadou [10,53], P. Hauer [42], S. Hayashi [132], S.T. Heckel [68,104], E. Hellbär [68], H. Helstrup [35], A. Herghelegiu [47], T. Herman [36], E.G. Hernandez [44], G. Herrera Corral [9], F. Herrmann [144], K.F. Hetland [35], T.E. Hilden [43], H. Hillemanns [33], C. Hills [127], B. Hippolyte [136], B. Hohlweger [104], D. Horak [36], A. Hornung [68], S. Hornung [106], R. Hosokawa [15,133], P. Hristov [33], C. Huang [61], C. Hughes [130], P. Huhn [68], T.J. Humanic [96], H. Hushnud [109], L.A. Husova [144], N. Hussain [41], S.A. Hussain [14], D. Hutter [38], J.P. Iddon [33,127], R. Ilkaev [108], M. Inaba [133], G.M. Innocenti [33], M. Ippolitov [87], A. Isakov [94], M.S. Islam [109], M. Ivanov [106], V. Ivanov [97], V. Izucheev [90], B. Jacak [79], N. Jacazio [53], P.M. Jacobs [79], S. Jadlovska [116], J. Jadlovsky [116], S. Jaelani [63], C. Jahnke [121], M.J. Jakubowska [142], M.A. Janik [142], T. Janson [74], M. Jercic [98], O. Jevons [110], M. Jin [125], F. Jonas [95,144], P.G. Jones [110], J. Jung [68], M. Jung [68], A. Jusko [110], P. Kalinak [64], A. Kalweit [33], V. Kaplin [92], S. Kar [6], A. Karasu Uysal [77], O. Karavichev [62], T. Karavicheva [62], P. Karczmarczyk [33], E. Karpechev [62], A. Kazantsev [87], U. Kebschull [74], R. Keidel [46], M. Keil [33], B. Ketzer [42], Z. Khabanova [89], A.M. Khan [6], S. Khan [16], S.A. Khan [141], A. Khanzadeev [97], Y. Kharlov [90], A. Khatun [16], A. Khuntia [118], B. Kileng [35], B. Kim [60], B. Kim [133], D. Kim [147], D.J. Kim [126], E.J. Kim [73], H. Kim [17,147], J. Kim [147], J.S. Kim [40], J. Kim [103], J. Kim [147], J. Kim [73], M. Kim [103], S. Kim [18], T. Kim [147], T. Kim [147], S. Kirsch [38,68], I. Kisel [38], S. Kiselev [91], A. Kisiel [142], J.L. Klay [5], C. Klein [68], J. Klein [58], S. Klein [79], C. Klein-Bösing [144], M. Kleiner [68], A. Kluge [33], M.L. Knichel [33], A.G. Knospe [125], C. Kobdaj [115], M.K. Köhler [103], T. Kollegger [106], A. Kondratyev [75], N. Kondratyeva [92], E. Kondratyuk [90], J. Konig [68], P.J. Konopka [33], L. Koska [116], O. Kovalenko [84], V. Kovalenko [112], M. Kowalski [118], I. Králik [64], A. Kravčáková [37], L. Kreis [106], M. Krivda [64,110], F. Krizek [94], K. Krizkova Gajdosova [36], M. Krüger [68], E. Kryshen [97], M. Krzewicki [38], A.M. Kubera [96], V. Kučera [60], C. Kuhn [136], P.G. Kuijer [89], L. Kumar [99], S. Kumar [48], S. Kundu [85], P. Kurashvili [84], A. Kurepin [62], A.B. Kurepin [62], A. Kuryakin [108], S. Kushpil [94], J. Kvapil [110], M.J. Kweon [60], J.Y. Kwon [60], Y. Kwon [147], S.L. La Pointe [38], P. La Rocca [27], P. Ladron de Guevara [71], Y.S. Lai [79], R. Langoy [129], K. Lapidus [33], A. Lardeux [20], P. Larionov [51], E. Laudi [33], R. Lavicka [36], T. Lazareva [112], R. Lea [24], L. Leardini [103], J. Lee [133], S. Lee [147], F. Lehas [89], S. Lehner [113], J. Lehrbach [38], R.C. Lemmon [93], I. León Monzón [120], E.D. Lesser [19], M. Lettrich [33], P. Lévai [145], X. Li [12], X.L. Li [6], J. Lien [129], R. Lietava [110], B. Lim [17], V. Lindenstruth [38], S.W. Lindsay [127], C. Lippmann [106], M.A. Lisa [96], V. Litichevskyi [43], A. Liu [19], S. Liu [96], W.J. Llope [143], I.M. Lofnes [21], V. Loginov [92], C. Loizides [95], P. Loncar [34], X. Lopez [134], E. López Torres [8], J.R. Luhder [144], M. Lunardon [28], G. Luparello [59], Y. Ma [39], A. Maevskaya [62], M. Mager [33], S.M. Mahmood [20], T. Mahmoud [42], A. Maire [136], R.D. Majka [146], M. Malaev [97], Q.W. Malik [20], L. Malinina [75,iii], D. Mal'Kevich [91], P. Malzacher [106], G. Mandaglio [55], V. Manko [87], F. Manso [134], V. Manzari [52], Y. Mao [6], M. Marchisone [135], J. Mareš [66], G.V. Margagliotti [24], A. Margotti [53], J. Margutti [63], A. Marín [106], C. Markert [119], M. Marquard [68], N.A. Martin [103], P. Martinengo [33], J.L. Martinez [125], M.I. Martínez [44], G. Martínez García [114], M. Martinez Pedreira [33], S. Masciocchi [106], M. Masera [25], A. Masoni [54], L. Massacrier [61], E. Masson [114], A. Mastroserio [52,138], A.M. Mathis [104,117], O. Matonoha [80], P.F.T. Matuoka [121], A. Matyja [118], C. Mayer [118], M. Mazzilli [52], M.A. Mazzoni [57], A.F. Mechler [68], F. Meddi [22], Y. Melikyan [62,92], A. Menchaca-Rocha [71], C. Mengke [6], E. Meninno [29,113], M. Meres [13], S. Mhlanga [124], Y. Miake [133], L. Micheletti [25], D.L. Mihaylov [104], K. Mikhaylov [75,91], A. Mischke [63,i], A.N. Mishra [69], D. Miśkowiec [106], A. Modak [3], N. Mohammadi [33], A.P. Mohanty [63], B. Mohanty [85], M. Mohisin Khan [16,iv], C. Mordasini [104], D.A. Moreira De Godoy [144], L.A.P. Moreno [44], I. Morozov [62], A. Morsch [33], T. Mrnjavac [33], V. Muccifora [51], E. Mudnic [34], D. Mühlheim [144], S. Muhuri [141], J.D. Mulligan [79], M.G. Munhoz [121], R.H. Munzer [68], H. Murakami [132], S. Murray [124], L. Musa [33], J. Musinsky [64], C.J. Myers [125], J.W. Myrcha [142], B. Naik [48],

R. Nair [84], B.K. Nandi [48], R. Nania [10,53], E. Nappi [52], M.U. Naru [14], A.F. Nassirpour [80], C. Nattrass [130], R. Nayak [48], T.K. Nayak [85], S. Nazarenko [108], A. Neagu [20], R.A. Negrao De Oliveira [68], L. Nellen [69], S.V. Nesbo [35], G. Neskovic [38], D. Nesterov [112], L.T. Neumann [142], B.S. Nielsen [88], S. Nikolaev [87], S. Nikulin [87], V. Nikulin [97], F. Noferini [10,53], P. Nomokonov [75], J. Norman [78,127], N. Novitzky [133], P. Nowakowski [142], A. Nyanin [87], J. Nystrand [21], M. Ogino [81], A. Ohlson [80,103], J. Oleniacz [142], A.C. Oliveira Da Silva [121,130], M.H. Oliver [146], C. Oppedisano [58], R. Orava [43], A. Ortiz Velasquez [69], A. Oskarsson [80], J. Otwinowski [118], K. Oyama [81], Y. Pachmayer [103], V. Pacik [88], D. Pagano [140], G. Paić [69], J. Pan [143], A.K. Pandey [48], S. Panebianco [137], P. Pareek [49,141], J. Park [60], J.E. Parkkila [126], S. Parmar [99], S.P. Pathak [125], R.N. Patra [141], B. Paul [23,58], H. Pei [6], T. Peitzmann [63], X. Peng [6], L.G. Pereira [70], H. Pereira Da Costa [137], D. Peresunko [87], G.M. Perez [8], E. Perez Lezama [68], V. Peskov [68], Y. Pestov [4], V. Petráček [36], M. Petrovici [47], R.P. Pezzi [70], S. Piano [59], M. Pikna [13], P. Pillot [114], O. Pinazza [33,53], L. Pinsky [125], C. Pinto [27], S. Pisano [10,51], D. Pistone [55], M. Płoskoń [79], M. Planinic [98], F. Pliquett [68], J. Pluta [142], S. Pochybova [145,i], M.G. Poghosyan [95], B. Polichtchouk [90], N. Poljak [98], A. Pop [47], H. Poppenborg [144], S. Porteboeuf-Houssais [134], V. Pozdniakov [75], S.K. Prasad [3], R. Preghenella [53], F. Prino [58], C.A. Pruneau [143], I. Pshenichnov [62], M. Puccio [25,33], J. Putschke [143], R.E. Quishpe [125], S. Ragoni [110], S. Raha [3], S. Rajput [100], J. Rak [126], A. Rakotozafindrabe [137], L. Ramello [31], F. Rami [136], R. Raniwala [101], S. Raniwala [101], S.S. Räsänen [43], R. Rath [49], V. Ratza [42], I. Ravasenga [30,89], K.F. Read [95,130], A.R. Redelbach [38], K. Redlich [84,v], A. Rehman [21], P. Reichelt [68], F. Reidt [33], X. Ren [6], R. Renfordt [68], Z. Rescakova [37], J.-P. Revol [10], K. Reygers [103], V. Riabov [97], T. Richert [80,88], M. Richter [20], P. Riedler [33], W. Riegler [33], F. Riggi [27], C. Ristea [67], S.P. Rode [49], M. Rodríguez Cahuantzi [44], K. Røed [20], R. Rogalev [90], E. Rogochaya [75], D. Rohr [33], D. Röhrich [21], P.S. Rokita [142], F. Ronchetti [51], E.D. Rosas [69], K. Roslon [142], A. Rossi [28,56], A. Rotondi [139], A. Roy [49], P. Roy [109], O.V. Rueda [80], R. Rui [24], B. Rumyantsev [75], A. Rustamov [86], E. Ryabinkin [87], Y. Ryabov [97], A. Rybicki [118], H. Rytkonen [126], O.A.M. Saarimaki [43], S. Sadhu [141], S. Sadovsky [90], K. Šafařík [36], S.K. Saha [141], B. Sahoo [48], P. Sahoo [48,49], R. Sahoo [49], S. Sahoo [65], P.K. Sahu [65], J. Saini [141], S. Sakai [133], S. Sambyal [100], V. Samsonov [92,97], D. Sarkar [143], N. Sarkar [141], P. Sarma [41], V.M. Sarti [104], M.H.P. Sas [63], E. Scapparone [53], B. Schaefer [95], J. Schambach [119], H.S. Scheid [68], C. Schiaua [47], R. Schicker [103], A. Schmah [103], C. Schmidt [106], H.R. Schmidt [102], M.O. Schmidt [103], M. Schmidt [102], N.V. Schmidt [68,95], A.R. Schmier [130], J. Schukraft [88], Y. Schutz [33,136], K. Schwarz [106], K. Schweda [106], G. Scioli [26], E. Scomparin [58], M. Šefčík [37], J.E. Seger [15], Y. Sekiguchi [132], D. Sekihata [132], I. Selyuzhenkov [92,106], S. Senyukov [136], D. Serebryakov [62], E. Serradilla [71], A. Sevcenco [67], A. Shabanov [62], A. Shabetai [114], R. Shahoyan [33], W. Shaikh [109], A. Shangaraev [90], A. Sharma [99], A. Sharma [100], H. Sharma [118], M. Sharma [100], N. Sharma [99], A.I. Sheikh [141], K. Shigaki [45], M. Shimomura [82], S. Shirinkin [91], Q. Shou [39], Y. Sibiriak [87], S. Siddhanta [54], T. Siemiarczuk [84], D. Silvermyr [80], G. Simatovic [89], G. Simonetti [33,104], R. Singh [85], R. Singh [100], R. Singh [49], V.K. Singh [141], V. Singhal [141], T. Sinha [109], B. Sitar [13], M. Sitta [31], T.B. Skaali [20], M. Slupecki [126], N. Smirnov [146], R.J.M. Snellings [63], T.W. Snellman [43,126], C. Soncco [111], J. Song [60,125], A. Songmoolnak [115], F. Soramel [28], S. Sorensen [130], I. Sputowska [118], J. Stachel [103], I. Stan [67], P. Stankus [95], P.J. Steffanic [130], E. Stenlund [80], D. Stocco [114], M.M. Storetvedt [35], L.D. Stritto [29], A.A.P. Suaide [121], T. Sugitate [45], C. Suire [61], M. Suleymanov [14], M. Suljic [33], R. Sultanov [91], M. Šumbera [94], S. Sumowidagdo [50], S. Swain [65], A. Szabo [13], I. Szarka [13], U. Tabassam [14], G. Taillepied [134], J. Takahashi [122], G.J. Tambave [21], S. Tang [6,134], M. Tarhini [114], M.G. Tarzila [47], A. Tauro [33], G. Tejeda Muñoz [44], A. Telesca [33], C. Terrevoli [125], D. Thakur [49], S. Thakur [141], D. Thomas [119], F. Thoresen [88], R. Tieulent [135], A. Tikhonov [62], A.R. Timmins [125], A. Toia [68], N. Topilskaya [62], M. Toppi [51], F. Torales-Acosta [19], S.R. Torres [9,120], A. Trifiro [55], S. Tripathy [49], T. Tripathy [48], S. Trogolo [28], G. Trombetta [32], L. Tropp [37], V. Trubnikov [2], W.H. Trzaska [126], T.P. Trzcinski [142], B.A. Trzeciak [63], T. Tsuji [132], A. Tumkin [108], R. Turrisi [56], T.S. Tveter [20], K. Ullaland [21], E.N. Umaka [125], A. Uras [135], G.L. Usai [23], A. Utrobicic [98], M. Vala [37], N. Valle [139], S. Vallero [58], N. van der Kolk [63], L.V.R. van Doremalen [63], M. van Leeuwen [63], P. Vande Vyvre [33], D. Varga [145], Z. Varga [145], M. Varga-Kofarago [145], A. Vargas [44], M. Vasileiou [83], A. Vasiliev [87], O. Vázquez Doce [104,117], V. Vechernin [112], A.M. Veen [63], E. Vercellin [25], S. Vergara Limón [44], L. Vermunt [63], R. Vernet [7], R. Vértesi [145], L. Vickovic [34], Z. Vilakazi [131], O. Villalobos Baillie [110], A. Villatoro Tello [44], G. Vino [52], A. Vinogradov [87], T. Virgili [29], V. Vislavicius [88], A. Vodopyanov [75], B. Volkel [33], M.A. Völkl [102], K. Voloshin [91], S.A. Voloshin [143], G. Volpe [32], B. von Haller [33], I. Vorobyev [104], D. Voscek [116], J. Vrláková [37], B. Wagner [21], M. Weber [113], S.G. Weber [144], A. Wegrzynek [33], D.F. Weiser [103], S.C. Wenzel [33],

J.P. Wessels [144], J. Wiechula [68], J. Wikne [20], G. Wilk [84], J. Wilkinson [10,53], G.A. Willems [33], E. Willsher [110], B. Windelband [103], M. Winn [137], W.E. Witt [130], Y. Wu [128], R. Xu [6], S. Yalcin [77], K. Yamakawa [45], S. Yang [21], S. Yano [137], Z. Yin [6], H. Yokoyama [63], I.-K. Yoo [17], J.H. Yoon [60], S. Yuan [21], A. Yuncu [103], V. Yurchenko [2], V. Zaccolo [24], A. Zaman [14], C. Zampolli [33], H.J.C. Zanoli [63], N. Zardoshti [33], A. Zarochentsev [112], P. Závada [66], N. Zaviyalov [108], H. Zbroszczyk [142], M. Zhalov [97], S. Zhang [39], X. Zhang [6], Z. Zhang [6], V. Zherebchevskii [112], D. Zhou [6], Y. Zhou [88], Z. Zhou [21], J. Zhu [6,106], Y. Zhu [6], A. Zichichi [10,26], M.B. Zimmermann [33], G. Zinovjev [2], N. Zurlo [140]

[1] *A.I. Alikhanyan National Science Laboratory (Yerevan Physics Institute) Foundation, Yerevan, Armenia*
[2] *Bogolyubov Institute for Theoretical Physics, National Academy of Sciences of Ukraine, Kiev, Ukraine*
[3] *Bose Institute, Department of Physics and Centre for Astroparticle Physics and Space Science (CAPSS), Kolkata, India*
[4] *Budker Institute for Nuclear Physics, Novosibirsk, Russia*
[5] *California Polytechnic State University, San Luis Obispo, CA, United States*
[6] *Central China Normal University, Wuhan, China*
[7] *Centre de Calcul de l'IN2P3, Villeurbanne, Lyon, France*
[8] *Centro de Aplicaciones Tecnológicas y Desarrollo Nuclear (CEADEN), Havana, Cuba*
[9] *Centro de Investigación y de Estudios Avanzados (CINVESTAV), Mexico City and Mérida, Mexico*
[10] *Centro Fermi - Museo Storico della Fisica e Centro Studi e Ricerche "Enrico Fermi", Rome, Italy*
[11] *Chicago State University, Chicago, IL, United States*
[12] *China Institute of Atomic Energy, Beijing, China*
[13] *Comenius University Bratislava, Faculty of Mathematics, Physics and Informatics, Bratislava, Slovakia*
[14] *COMSATS University Islamabad, Islamabad, Pakistan*
[15] *Creighton University, Omaha, NE, United States*
[16] *Department of Physics, Aligarh Muslim University, Aligarh, India*
[17] *Department of Physics, Pusan National University, Pusan, Republic of Korea*
[18] *Department of Physics, Sejong University, Seoul, Republic of Korea*
[19] *Department of Physics, University of California, Berkeley, CA, United States*
[20] *Department of Physics, University of Oslo, Oslo, Norway*
[21] *Department of Physics and Technology, University of Bergen, Bergen, Norway*
[22] *Dipartimento di Fisica dell'Università 'La Sapienza' and Sezione INFN, Rome, Italy*
[23] *Dipartimento di Fisica dell'Università and Sezione INFN, Cagliari, Italy*
[24] *Dipartimento di Fisica dell'Università and Sezione INFN, Trieste, Italy*
[25] *Dipartimento di Fisica dell'Università and Sezione INFN, Turin, Italy*
[26] *Dipartimento di Fisica e Astronomia dell'Università and Sezione INFN, Bologna, Italy*
[27] *Dipartimento di Fisica e Astronomia dell'Università and Sezione INFN, Catania, Italy*
[28] *Dipartimento di Fisica e Astronomia dell'Università and Sezione INFN, Padova, Italy*
[29] *Dipartimento di Fisica 'E.R. Caianiello' dell'Università and Gruppo Collegato INFN, Salerno, Italy*
[30] *Dipartimento DISAT del Politecnico and Sezione INFN, Turin, Italy*
[31] *Dipartimento di Scienze e Innovazione Tecnologica dell'Università del Piemonte Orientale and INFN Sezione di Torino, Alessandria, Italy*
[32] *Dipartimento Interateneo di Fisica 'M. Merlin' and Sezione INFN, Bari, Italy*
[33] *European Organization for Nuclear Research (CERN), Geneva, Switzerland*
[34] *Faculty of Electrical Engineering, Mechanical Engineering and Naval Architecture, University of Split, Split, Croatia*
[35] *Faculty of Engineering and Science, Western Norway University of Applied Sciences, Bergen, Norway*
[36] *Faculty of Nuclear Sciences and Physical Engineering, Czech Technical University in Prague, Prague, Czech Republic*
[37] *Faculty of Science, P.J. Šafárik University, Košice, Slovakia*
[38] *Frankfurt Institute for Advanced Studies, Johann Wolfgang Goethe-Universität Frankfurt, Frankfurt, Germany*
[39] *Fudan University, Shanghai, China*
[40] *Gangneung-Wonju National University, Gangneung, Republic of Korea*
[41] *Gauhati University, Department of Physics, Guwahati, India*
[42] *Helmholtz-Institut für Strahlen- und Kernphysik, Rheinische Friedrich-Wilhelms-Universität Bonn, Bonn, Germany*
[43] *Helsinki Institute of Physics (HIP), Helsinki, Finland*
[44] *High Energy Physics Group, Universidad Autónoma de Puebla, Puebla, Mexico*
[45] *Hiroshima University, Hiroshima, Japan*
[46] *Hochschule Worms, Zentrum für Technologietransfer und Telekommunikation (ZTT), Worms, Germany*
[47] *Horia Hulubei National Institute of Physics and Nuclear Engineering, Bucharest, Romania*
[48] *Indian Institute of Technology Bombay (IIT), Mumbai, India*
[49] *Indian Institute of Technology Indore, Indore, India*
[50] *Indonesian Institute of Sciences, Jakarta, Indonesia*
[51] *INFN, Laboratori Nazionali di Frascati, Frascati, Italy*
[52] *INFN, Sezione di Bari, Bari, Italy*
[53] *INFN, Sezione di Bologna, Bologna, Italy*
[54] *INFN, Sezione di Cagliari, Cagliari, Italy*
[55] *INFN, Sezione di Catania, Catania, Italy*
[56] *INFN, Sezione di Padova, Padova, Italy*
[57] *INFN, Sezione di Roma, Rome, Italy*
[58] *INFN, Sezione di Torino, Turin, Italy*
[59] *INFN, Sezione di Trieste, Trieste, Italy*
[60] *Inha University, Incheon, Republic of Korea*
[61] *Institut de Physique Nucléaire d'Orsay (IPNO), Institut National de Physique Nucléaire et de Physique des Particules (IN2P3/CNRS), Université de Paris-Sud, Université Paris-Saclay, Orsay, France*
[62] *Institute for Nuclear Research, Academy of Sciences, Moscow, Russia*
[63] *Institute for Subatomic Physics, Utrecht University/Nikhef, Utrecht, Netherlands*
[64] *Institute of Experimental Physics, Slovak Academy of Sciences, Košice, Slovakia*
[65] *Institute of Physics, Homi Bhabha National Institute, Bhubaneswar, India*
[66] *Institute of Physics of the Czech Academy of Sciences, Prague, Czech Republic*
[67] *Institute of Space Science (ISS), Bucharest, Romania*
[68] *Institut für Kernphysik, Johann Wolfgang Goethe-Universität Frankfurt, Frankfurt, Germany*

[69] Instituto de Ciencias Nucleares, Universidad Nacional Autónoma de México, Mexico City, Mexico
[70] Instituto de Física, Universidade Federal do Rio Grande do Sul (UFRGS), Porto Alegre, Brazil
[71] Instituto de Física, Universidad Nacional Autónoma de México, Mexico City, Mexico
[72] iThemba LABS, National Research Foundation, Somerset West, South Africa
[73] Jeonbuk National University, Jeonju, Republic of Korea
[74] Johann-Wolfgang-Goethe Universität Frankfurt Institut für Informatik, Fachbereich Informatik und Mathematik, Frankfurt, Germany
[75] Joint Institute for Nuclear Research (JINR), Dubna, Russia
[76] Korea Institute of Science and Technology Information, Daejeon, Republic of Korea
[77] KTO Karatay University, Konya, Turkey
[78] Laboratoire de Physique Subatomique et de Cosmologie, Université Grenoble-Alpes, CNRS-IN2P3, Grenoble, France
[79] Lawrence Berkeley National Laboratory, Berkeley, CA, United States
[80] Lund University Department of Physics, Division of Particle Physics, Lund, Sweden
[81] Nagasaki Institute of Applied Science, Nagasaki, Japan
[82] Nara Women's University (NWU), Nara, Japan
[83] National and Kapodistrian University of Athens, School of Science, Department of Physics, Athens, Greece
[84] National Centre for Nuclear Research, Warsaw, Poland
[85] National Institute of Science Education and Research, Homi Bhabha National Institute, Jatni, India
[86] National Nuclear Research Center, Baku, Azerbaijan
[87] National Research Centre Kurchatov Institute, Moscow, Russia
[88] Niels Bohr Institute, University of Copenhagen, Copenhagen, Denmark
[89] Nikhef, National institute for subatomic physics, Amsterdam, Netherlands
[90] NRC Kurchatov Institute IHEP, Protvino, Russia
[91] NRC Kurchatov Institute - ITEP, Moscow, Russia
[92] NRNU Moscow Engineering Physics Institute, Moscow, Russia
[93] Nuclear Physics Group, STFC Daresbury Laboratory, Daresbury, United Kingdom
[94] Nuclear Physics Institute of the Czech Academy of Sciences, Řež u Prahy, Czech Republic
[95] Oak Ridge National Laboratory, Oak Ridge, TN, United States
[96] Ohio State University, Columbus, OH, United States
[97] Petersburg Nuclear Physics Institute, Gatchina, Russia
[98] Physics department, Faculty of Science, University of Zagreb, Zagreb, Croatia
[99] Physics Department, Panjab University, Chandigarh, India
[100] Physics Department, University of Jammu, Jammu, India
[101] Physics Department, University of Rajasthan, Jaipur, India
[102] Physikalisches Institut, Eberhard-Karls-Universität Tübingen, Tübingen, Germany
[103] Physikalisches Institut, Ruprecht-Karls-Universität Heidelberg, Heidelberg, Germany
[104] Physik Department, Technische Universität München, Munich, Germany
[105] Politecnico di Bari, Bari, Italy
[106] Research Division and ExtreMe Matter Institute EMMI, GSI Helmholtzzentrum für Schwerionenforschung GmbH, Darmstadt, Germany
[107] Rudjer Bošković Institute, Zagreb, Croatia
[108] Russian Federal Nuclear Center (VNIIEF), Sarov, Russia
[109] Saha Institute of Nuclear Physics, Homi Bhabha National Institute, Kolkata, India
[110] School of Physics and Astronomy, University of Birmingham, Birmingham, United Kingdom
[111] Sección Física, Departamento de Ciencias, Pontificia Universidad Católica del Perú, Lima, Peru
[112] St. Petersburg State University, St. Petersburg, Russia
[113] Stefan Meyer Institut für Subatomare Physik (SMI), Vienna, Austria
[114] SUBATECH, IMT Atlantique, Université de Nantes, CNRS-IN2P3, Nantes, France
[115] Suranaree University of Technology, Nakhon Ratchasima, Thailand
[116] Technical University of Košice, Košice, Slovakia
[117] Technische Universität München, Excellence Cluster 'Universe', Munich, Germany
[118] The Henryk Niewodniczanski Institute of Nuclear Physics, Polish Academy of Sciences, Cracow, Poland
[119] The University of Texas at Austin, Austin, TX, United States
[120] Universidad Autónoma de Sinaloa, Culiacán, Mexico
[121] Universidade de São Paulo (USP), São Paulo, Brazil
[122] Universidade Estadual de Campinas (UNICAMP), Campinas, Brazil
[123] Universidade Federal do ABC, Santo Andre, Brazil
[124] University of Cape Town, Cape Town, South Africa
[125] University of Houston, Houston, TX, United States
[126] University of Jyväskylä, Jyväskylä, Finland
[127] University of Liverpool, Liverpool, United Kingdom
[128] University of Science and Technology of China, Hefei, China
[129] University of South-Eastern Norway, Tonsberg, Norway
[130] University of Tennessee, Knoxville, TN, United States
[131] University of the Witwatersrand, Johannesburg, South Africa
[132] University of Tokyo, Tokyo, Japan
[133] University of Tsukuba, Tsukuba, Japan
[134] Université Clermont Auvergne, CNRS/IN2P3, LPC, Clermont-Ferrand, France
[135] Université de Lyon, Université Lyon 1, CNRS/IN2P3, IPN-Lyon, Villeurbanne, Lyon, France
[136] Université de Strasbourg, CNRS, IPHC UMR 7178, F-67000 Strasbourg, France
[137] Université Paris-Saclay Centre d'Etudes de Saclay (CEA), IRFU, Départment de Physique Nucléaire (DPhN), Saclay, France
[138] Università degli Studi di Foggia, Foggia, Italy
[139] Università degli Studi di Pavia, Pavia, Italy
[140] Università di Brescia, Brescia, Italy
[141] Variable Energy Cyclotron Centre, Homi Bhabha National Institute, Kolkata, India
[142] Warsaw University of Technology, Warsaw, Poland
[143] Wayne State University, Detroit, MI, United States
[144] Westfälische Wilhelms-Universität Münster, Institut für Kernphysik, Münster, Germany
[145] Wigner Research Centre for Physics, Budapest, Hungary
[146] Yale University, New Haven, CT, United States
[147] Yonsei University, Seoul, Republic of Korea

[i] Deceased.
[ii] Dipartimento DET del Politecnico di Torino, Turin, Italy.
[iii] M.V. Lomonosov Moscow State University, D.V. Skobeltsyn Institute of Nuclear, Physics, Moscow, Russia.
[iv] Department of Applied Physics, Aligarh Muslim University, Aligarh, India.
[v] Institute of Theoretical Physics, University of Wroclaw, Poland.